Solution of Navier-Stokes equations by fourth-order compact schemes and AUSM flux splitting

Mahmood K. Mawlood
Department of Mechanical Engineering, Faculty of Engineering, Universiti Tenaga Nasional, Selangor, Malaysia

Shahnor Basri
Department of Aerospace Engineering, Faculty of Engineering, Universiti Putra Malaysia, Selangor, Malaysia

Waqar Asrar and Ashraf A. Omar
Department of Mechanical Engineering, Faculty of Engineering, International Islamic University, Kuala Lumpur, Malaysia

Ahmad S. Mokhtar
Department of Aerospace Engineering, Faculty of Engineering, Universiti Putra Malaysia, Selangor, Malaysia, and

Megat M.H.M. Ahmad
Department of Mechanical Engineering, Faculty of Engineering, Universiti Putra Malaysia, Selangor, Malaysia

Received December 2003
Revised May 2005
Accepted May 2005

Abstract

Purpose – To develop a high-order compact finite-difference method for solving flow problems containing shock waves.

Design/methodology/approach – A numerical algorithm based on high-order compact finite-difference schemes is developed for solving Navier-Stokes equations in two-dimensional space. The convective flux terms are discretized by using advection upstream splitting method (AUSM). The developed method is then used to compute some example laminar flow problems. The problems considered have a range of Mach number that corresponds to subsonic incompressible flow to hypersonic compressible flows that contain shock waves and shock/boundary-layer interaction.

Findings – The paper shows that the AUSM flux splitting and high-order compact finite-difference methods can be used accurately and robustly in resolving shear layers and capturing shock waves. The highly diffusive nature of conventional flux splitting especially on coarse grids makes them inaccurate for boundary layers even with high-order discretization.

Originality/value – This paper presents a high-order numerical method that can accurately and robustly capture shock waves without deteriorating oscillations and resolve boundary layers and shock/boundary layer interaction.

Keywords Flow, Wave properties, Finite difference methods

Paper type Research paper

International Journal of Numerical Methods for Heat & Fluid Flow
Vol. 16 No. 1, 2006
pp. 107-120

0961-5539
DOI 10.1108/09615530610636982

Introduction

The primary objective of numerical schemes for solving practical application gas dynamics problems is to maximize both robustness and accuracy. This requirement is particularly important in full Navier-Stokes solutions in high-speed regimes where intense shock waves and boundary layers may simultaneously exist. High-order compact space discretization schemes have attracted much attention in recent years due to their narrow grid stencil, enhanced accuracy and better resolution characteristics over the non-compact conventional schemes.

Lele (1992) has presented and analyzed a class of high-order compact schemes for space discretization and introduced the notion of resolution efficiency. Wilson *et al.* (1998) have proposed high-order compact schemes and discussed their application to incompressible Navier-Stokes equations calculations. Ekaterinaris (1999, 2000) has discussed the application of central high-order compact schemes to Euler and compressible Navier-Stokes equations and developed implicit solution algorithms.

Upwind schemes are today's main trend of spatial discretization which may be categorized as either flux vector splitting (FVS) or flux difference splitting (FDS). FVS such as Steger and Warming's (1981) and Van Leer's (1979) are known to be simple and robust in the capture of intense shocks and rarefaction waves. The high-order compact methods developed by Cockburn and Shu (1994), Mawlood *et al.* (2003) and Ravichandran (1997) among others, are examples of FVS-based schemes. The drawback of FVS methods is that they have accuracy problems in resolving shear layer regions due to the excessive numerical dissipation error associated with them.

In contrast, FDS such as Roe's (1981) scheme that utilizes the solution of the local Riemann problem usually provides accurate solutions. The numerical methods developed by Deng and Maekawa (1997) for solving Euler equations and Deng and Zhang (2000) for Euler and Navier-Stokes equations are examples of high-order compact methods that utilize Roe's (1981) FDS. Unfortunately, Roe's scheme has a number of robustness problems such as the violation of entropy condition and the carbuncle phenomenon (Liou and Steffen, 1993).

A recent trend in the development of upwind schemes has centered on the construction of hybrid flux-splitting formulations which seek to combine the accuracy of FDS approaches in the resolution of shear layers with the robustness of FVS in the capturing of strong discontinuities. Liou and Steffen (1993) among others, suggested a method known as the advection upstream splitting method (AUSM). In this method, the inviscid flux at a cell interface is split into a convective contribution, which is upwinded in the direction of the flow, and a pressure contribution, which is upwinded based on acoustic considerations. The direction of the flow is determined by the sign of a Mach number defined by combining information from both the left and right states about the cell interface.

In the present work, a fourth-order compact space discretization method that is based on the AUSM flux splitting is developed and tested. The method is used for the discretization of the convective flux terms of the Navier-Stokes equations. The diffusive flux terms of the Navier-Stokes equations are discretized by a central fourth-order compact method. Computed results are presented for four example problems, namely, incompressible laminar flow between parallel plates, shock-boundary layer interaction, hypersonic flow past 24° compression ramp and hypersonic flow past a circular cylinder. In the first example, a comparison is made

between Van Leer's FVS and AUSM results on a coarse grid. The tests have shown that the AUSM-based method resolves the shear layer and its development very well. The computed results for the shock-boundary layer interaction and the hypersonic flows compare favorably with the available experimental and numerical data. The computed results also indicate that FVS method is inadequate for computing shear layers with coarse grid and that the highly diffusive nature of FVS cannot be cured by high-order accurate schemes.

Governing equations

The two-dimensional normalized compressible Navier-Stokes equations can be written in the strong conservation form as

$$\frac{\partial Q}{\partial t}+\frac{\partial E}{\partial x}+\frac{\partial F}{\partial y}=\frac{\partial E_v}{\partial x}+\frac{\partial F_v}{\partial y} \tag{1}$$

where

$$Q=\begin{bmatrix}\rho\\ \rho u\\ \rho v\\ \rho e\end{bmatrix},\quad E=\begin{bmatrix}\rho u\\ \rho u^2+p\\ \rho uv\\ \rho uH\end{bmatrix},\quad F=\begin{bmatrix}\rho u\\ \rho uv\\ \rho v^2+p\\ \rho vH\end{bmatrix}$$

$$E_v=\frac{1}{Re_c}\begin{bmatrix}0\\ \tau_{xx}\\ \tau_{xy}\\ u\tau_{xx}+v\tau_{xy}-q_x\end{bmatrix},\quad F_v=\frac{1}{Re_c}\begin{bmatrix}0\\ \tau_{xy}\\ \tau_{yy}\\ u\tau_{xy}+v\tau_{yy}-q_y\end{bmatrix}$$

$$\tau_{ij}=2\mu\left(S_{ij}-\frac{S_{kk}\delta_{ij}}{3}\right)$$

$$S_{ij}=\frac{1}{2}\left(\frac{\partial u_i}{\partial x_j}+\frac{\partial u_j}{\partial x_i}\right)$$

$$q_j=-\frac{\mu}{Pr(\gamma-1)}\frac{\partial T}{\partial x_j}$$

here ρ, u, v, p, e and H are the density, the x-component of velocity, the y-component of velocity, the pressure, the total energy, and the total enthalpy, respectively. The total enthalpy H, is related to the other quantities by the relation

$$H=e+\frac{p}{\rho}.$$

For a perfect gas the total energy is given by

$$e = \frac{p}{\rho(\gamma - 1)} + \frac{1}{2}(u^2 + v^2)$$

where γ is the ratio of specific heats and takes the value of 1.4 for air. The normalization has been carried out by using the following free-stream reference quantities: density ρ_∞, sonic speed c_∞, pressure $\rho_\infty c_\infty^2$, reference length scale L_∞ and the reference time L_∞/c_∞. The sonic speed is defined as $c = \sqrt{\gamma p/\rho}$.

Equation (1) can be transformed from Cartesian coordinates (x,y) into generalized coordinates (ξ, η) as

$$\frac{\partial \tilde{Q}}{\partial t} + \frac{\partial \tilde{E}}{\partial \xi} + \frac{\partial \tilde{F}}{\partial \eta} = \frac{\partial \tilde{E}_v}{\partial \xi} + \frac{\partial \tilde{F}_v}{\partial \eta} \tag{2}$$

where

$$\tilde{Q} = \frac{Q}{J},$$
$$\tilde{E} = \frac{(\xi_x E + \xi_y F)}{J},$$
$$\tilde{F} = \frac{(\eta_x E + \eta_y F)}{J}.$$

$$\tilde{E}_v = \frac{1}{J}(\xi_x E_v + \xi_y F_v),$$
$$\tilde{F}_v = \frac{1}{J}(\eta_x E_v + \eta_y F_v).$$

The metric terms are related to the derivatives of x and y by

$$\xi_x = J y_\eta, \quad \xi_y = -J x_\eta \eta_x = -J y_\xi, \quad \eta_y = J x_\xi \tag{3}$$

and the Jacobian of the transformation is given by

$$J = \frac{1}{(x_\xi y_\eta - y_\xi x_\eta)}. \tag{4}$$

Spatial discretization

It has been pointed out that FVS leads to excessive numerical diffusion and artificial broadening of boundary layers that cannot be cured by high-order differencing. Therefore, the hybrid AUSM flux splitting is adopted here for the discretization of the inviscid flux derivatives of the Navier-Stokes equations. In the following development the ξ-direction discretization is presented, the η-direction discretization follows a similar procedure. The mid-point numerical flux, using the AUSM splitting approach, can be written as (Liou and Steffen, 1993)

$$\tilde{E}_{i+1/2,j} = \frac{M_{1/2}\sqrt{\xi_x^2+\xi_y^2}}{J}\left(\begin{Bmatrix}\rho c\\ \rho uc\\ \rho vc\\ \rho Hc\end{Bmatrix}_L + \begin{Bmatrix}\rho c\\ \rho uc\\ \rho vc\\ \rho Hc\end{Bmatrix}_R\right) - \frac{|M_{1/2}|\sqrt{\xi_x^2+\xi_y^2}}{J}\left(\begin{Bmatrix}\rho c\\ \rho uc\\ \rho vc\\ \rho Hc\end{Bmatrix}_R - \begin{Bmatrix}\rho c\\ \rho uc\\ \rho vc\\ \rho Hc\end{Bmatrix}_L\right) + \frac{1}{J}\left(p_\xi^+\begin{Bmatrix}0\\ \xi_x p\\ \xi_y p\\ 0\end{Bmatrix}_L + p_\xi^-\begin{Bmatrix}0\\ \xi_x p\\ \xi_y p\\ 0\end{Bmatrix}_R\right) \tag{5}$$

where

$$M_{1/2} = \frac{\left(M_{\xi_L}^+ + M_{\xi_R}^-\right)}{2}$$

$M_\xi^\pm$ and $p_\xi^\pm$ are defined as follows:

$$M_\xi^\pm = \begin{cases} \pm\dfrac{1}{4}(M_\xi \pm 1)^2, & \text{if } |M_\xi| \le 1;\\ \dfrac{1}{2}\dfrac{(M_\xi \pm |M_\xi|)}{M_\xi} & \text{otherwise.}\end{cases}$$

$$p_\xi^\pm = \begin{cases} \dfrac{1}{2}(M_\xi \pm 1)^2(2 \mp M_\xi), & \text{if } |M_\xi| \le 1;\\ \dfrac{1}{2}\dfrac{(M_\xi \pm |M_\xi|)}{M_\xi}, & \text{otherwise.}\end{cases}$$

The left $(\cdot)_L$ and right $(\cdot)_R$ states are obtained by a fourth-order MUSCL polynomial presented by Yamamoto and Daiguji (1993). The high-order approximations to the derivatives are then obtained by the cell-centered fourth-order compact scheme of Lele (1992) as follows:

$$\frac{1}{22}\tilde{E}'_{i-1,j} + \tilde{E}'_{i,j} + \frac{1}{22}\tilde{E}'_{i+1,j} = \frac{24}{22\Delta\xi}(\tilde{E}_{i+1/2,j} - \tilde{E}_{i-1/2,j}) \tag{6}$$

where $\tilde{E}'_{i,j}$ represents the higher-order approximation to the first derivatives. Equation (6) is used for evaluating the derivatives at the interior points. At the boundaries the following one-sided compact schemes are used:

$$\tilde{E}'_{1,j} - \tilde{E}'_{2,j} = \frac{1}{\Delta\xi}(-\tilde{E}_{3/2,j} + 2\tilde{E}_{5/2,j} - \tilde{E}_{7/2,j}) \tag{7}$$

$$\tilde{E}'_{i\max,j} - \tilde{E}'_{i\max-1,j} = \frac{1}{\Delta\xi}(\tilde{E}_{i\max-1/2,j} - 2\tilde{E}_{i\max-3/2,j} + \tilde{E}_{i\max-5/2,j}). \tag{8}$$

Evaluation of the η-direction derivatives are carried out in a similar manner and are not shown here.

The computation of the viscous flux derivatives is carried out by a fourth-order compact central (Padé) scheme (Lele, 1992). The primitive variables u, v and T are first differentiated and the stress tensor is formed at each grid point. The viscous terms are then differentiated by another application of the compact scheme that can be written as (Lele, 1992)

$$15\tilde{E}'_{v_{i-1,j}} + 60\tilde{E}'_{v_{i,j}} + 15\tilde{E}'_{v_{i+1,j}} = \frac{45(\tilde{E}_{v_{i+1,j}} - \tilde{E}_{v_{i-1,j}})}{\Delta\xi} \tag{9}$$

$$15\tilde{F}'_{v_{i,j-1}} + 60\tilde{F}'_{v_{i,j}} + 15\tilde{F}'_{v_{i,j+1}} = \frac{45(\tilde{F}_{vi,j+1} - \tilde{F}_{v_{i,j-1}})}{\Delta\eta} \tag{10}$$

where $\tilde{E}'_{v_{i,j}}$ and $\tilde{F}'_{v_{i,j}}$ represent the fourth-order approximations to the derivatives $\partial\tilde{E}_v/\partial\xi|_{i,j}$ and $\partial\tilde{F}_v/\partial\eta|_{i,j}$, respectively.

Numerical results

Calculations are carried out for four laminar flow example problems with a Mach number range corresponding to subsonic incompressible flow up to compressible hypersonic flows. The first example is laminar incompressible flow between two parallel plates. It is intended to demonstrate the high diffusive nature of flux-vector splitting when used with coarse computational grid. Example 2 is shock boundary layer interaction past a flat plate, Example 3 is hypersonic flow past 24° ramp and Example 5 is hypersonic flow past a circular cylinder.

Example 1: incompressible laminar flow in a 2D channel

This test example as mentioned above, is intended to demonstrate the accuracy of the AUSM based high-order compact method developed in this study over the conventional Van Leer's FVS-based method. The diffusive nature of flux-vector splitting which makes it inadequate for viscous flow computation is demonstrated by using coarse mesh near the walls.

The exact solution of this flow problem in the fully developed region provides a benchmark for comparing the conventional van Leer's flux-vector splitting and the AUSM methods. At the inlet uniform velocity and density are specified $(\rho, u, v, p)_{\text{in}} = (1, 0.2, 0, p_{\text{extrap}})$ while the pressure is extrapolated from the interior points. At the outlet the pressure is specified ($p_{\text{out}} = 1/1.4$) and the derivatives of the other variables with respect to x are set to zero. Reynolds number ($Re = VL_\infty/\nu$) and Mach number M_{in} are set to 20 and 0.2, respectively. For this Reynolds number the expected length of the developing zone is

about $x/L_\infty \approx 1.2$. Therefore, a computational domain extending to $x/L_\infty = 2$ is considered in this test. The computational mesh is composed of (33 × 33) grid points distributed uniformly in the x- and y-directions as shown in Figure 1.

Figure 2 shows the variation of the computed normalized centerline velocity u_{max}/V with x/L_∞. The exact value in the fully developed zone ($u_{max}/V = 1.5$) is also shown. The AUSM method produces quite accurate value of the centerline velocity as the fully developed zone is approached. The van Leer's method overestimates the centerline velocity. The reason is that the excessive diffusion added by the flux-vector splitting method causes the boundary layer to grow thicker than its normal thickness.

The computed u-component velocity profiles in the fully developed zone ($x/L_\infty = 1.8$) are shown in Figure 3 in comparison with the exact parabolic velocity profile. Again the diffusive nature of the flux-vector splitting is very clear.

Example 2: shock-wave/boundary-layer interaction

In this test case, an oblique shock wave is made to impinge on a laminar boundary layer that has been developing on a flat plate. A strong shock with large incident angle causes

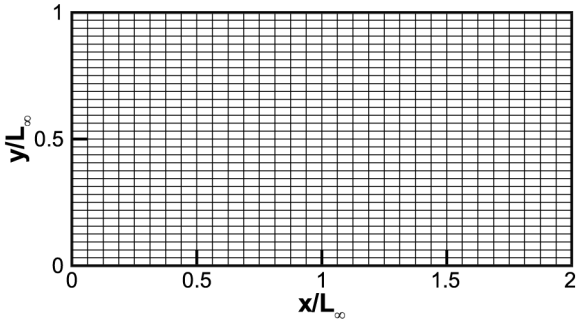

Figure 1.
Solution domain for laminar flow between parallel plates

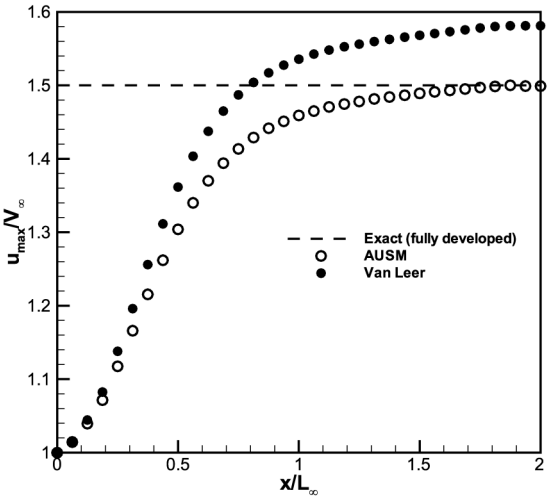

Figure 2.
Centerline velocity for laminar flow between parallel plates

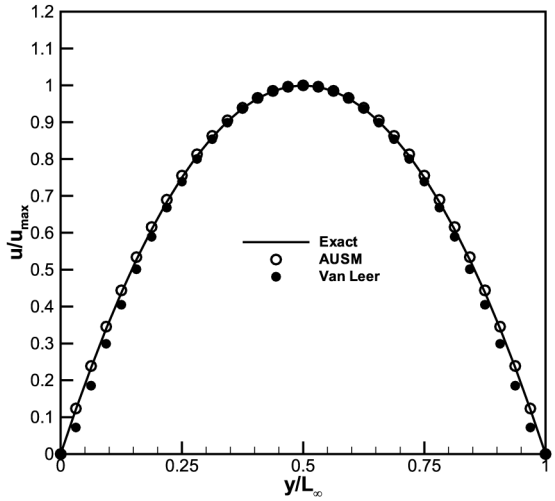

Figure 3.
Comparison of velocity profiles at $x/L_\infty = 1.8$ for laminar flow

the boundary layer to separate at the shock impinging point and subsequently it reattaches thus creating a separation bubble while maintaining laminar flow conditions throughout. The Mach number upstream the shock is $M_\infty = 2.0$, the corresponding shock angle is 32.58°, the Reynolds number $Re_\infty = 2.96 \times 10^5$ based on the upstream velocity and the shock impingement distance on the flat plate for an inviscid flow. A schematic diagram of the flow geometry is shown in Figure 4. Computations are carried out on a mesh with (121 × 81) grid points that are uniform in the stream-wise direction but clustered in the transverse direction close to the flat plate.

The computational flow features are shown by the pressure contours in Figure 5, which indicate the presence of a weak leading-edge shock generated by the initial growth of the boundary layer, compression waves created by the separated portion of the boundary layer, expansion waves over the separation bubble and recompression waves due to reattachment at the wall.

Figures 6 and 7 show the distributions for the coefficient of surface pressure, C_p, and the coefficient of skin-friction, C_f, respectively, in comparison with the experimental data (Hakkinen *et al.*, 1957). The filled symbols in Figure 7 representing experimental data of negative values for the C_f in the separated flow region indicate that their magnitudes have not be measured and have been set to zero for convenience. The numerical results including the separation location and length compare favorably with the experimental data.

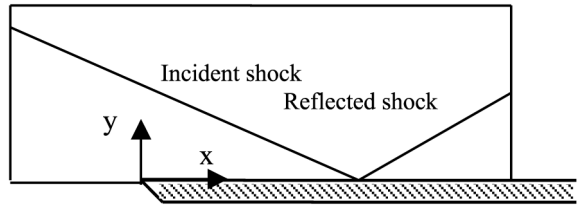

Figure 4.
Schematic of shock/boundary-layer interaction

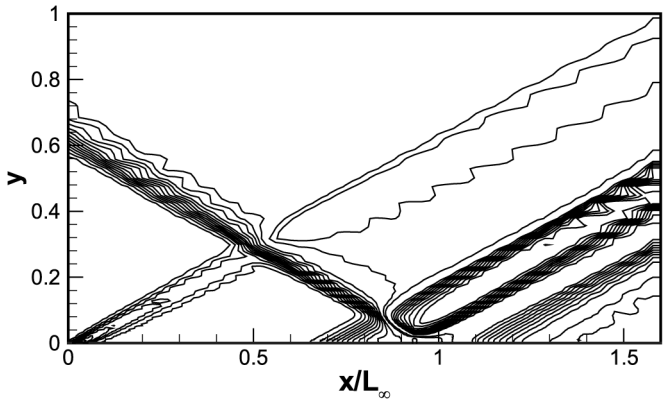

Figure 5.
Pressure contours for shock/boundary-layer interaction

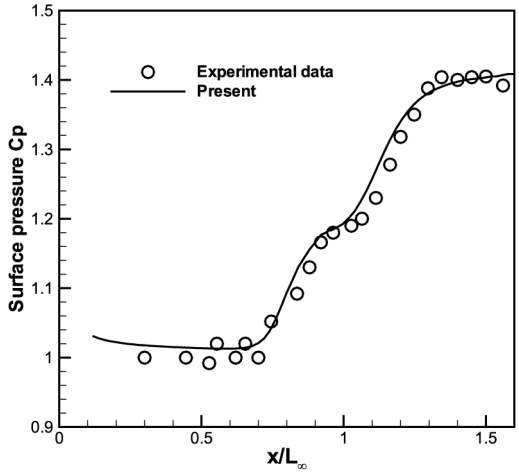

Figure 6.
Surface pressure coefficient C_p for shock/boundary-layer interaction

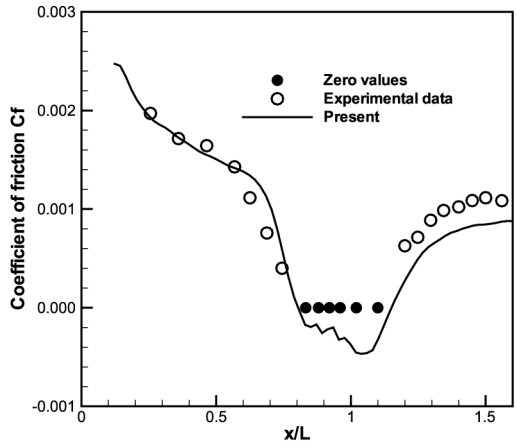

Figure 7.
Coefficient of friction for shock/boundary-layer interaction

Example 3: hypersonic flow past 24° compression ramp

In a hypersonic flow, the distribution of heat-transfer coefficient in addition to the distributions of surface pressure and skin-friction coefficients is required for assessing the accuracy of a numerical method.

The experimental data quoted by Kim *et al.* (1998) are used for testing the present method. A compression corner is formed at the junction of a flat plate and a ramp with 24° compression angle. The flow geometry and the grid are shown in Figure 8. The computational grid consists of (121 × 51) points that are uniform in the stream-wise direction but clustered in the transverse direction.

The free-stream conditions are as follows: Mach number $M_\infty = 14.1$, static gas temperature $T_\infty = 72.2\,\mathrm{K}$ which is low enough that real gas effects become unimportant, gas density $\rho_\infty = 4.84 \times 10^{-4}\,\mathrm{kg/m^3}$, static pressure $p_\infty = 10.1\,\mathrm{Pa}$, the absolute viscosity $\mu_\infty = 4.9369 \times 10^{-6}\,\mathrm{Pa\,s}$ and Reynolds number $Re_\infty = 1.04 \times 10^5$. The Reynolds number is based on the upstream velocity and the length of the flat portion of the compression corner. The wall condition is isothermal wall maintained at $T_\mathrm{w} = 297\,\mathrm{K}$.

The computed flow field as shown by the pressure contours in Figure 9, contains complicated shock-shock as well as shock boundary layer interactions. A leading-edge shock wave intersects an induced shock wave, generated by the turning of the boundary layer near the junction, to form a resultant shock accompanied by an expansion fan and contact surface all of which influence the flow field.

The computed values of the surface pressure coefficient, skin friction coefficient and the heat transfer coefficient represented by the Stanton number St are shown in Figures 10-12, respectively. From all the comparisons shown it can be observed that the calculations agree very well with the experimental data.

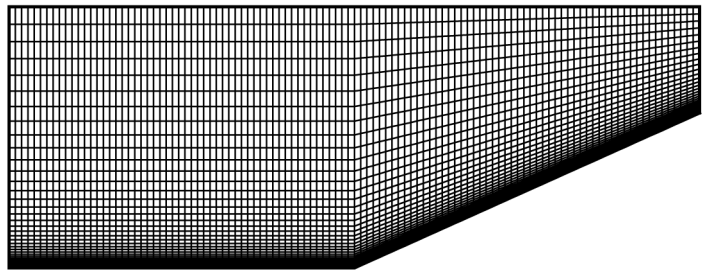

Figure 8.
Grid for hypersonic flow past a 24° ramp

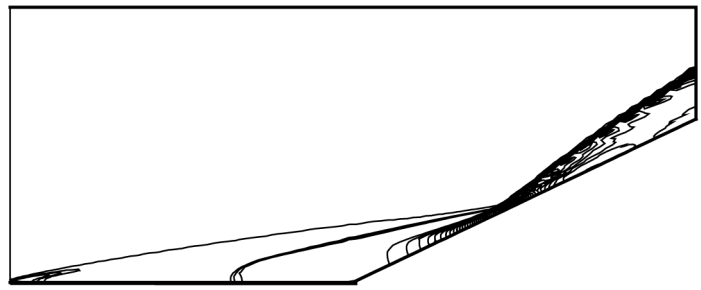

Figure 9.
Pressure contours for hypersonic flow past 24° ramp

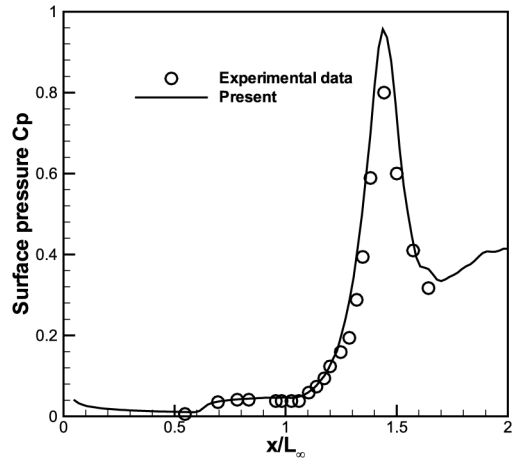

Figure 10.
Pressure coefficient for hypersonic flow past 24° ramp

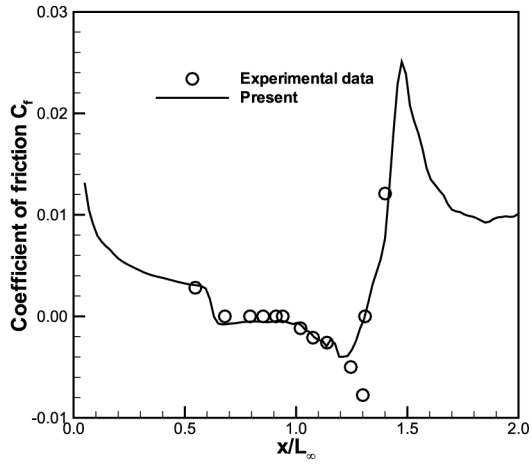

Figure 11.
Coefficient of friction for hypersonic flow past 24° ramp

Example 4: hypersonic flow past a circular cylinder

The last example is also steady hypersonic viscous flow but around a circular cylinder. In this example, the present results are compared with a spectral solution (Kopriva, 1993). The flow conditions are $M_\infty = 5.73$, $Re = 2{,}050$, $T_\infty = 39.6698\,\mathrm{K}$, $T_\mathrm{w} = 210.2\,\mathrm{K}$, $Pr = 0.77$ and the cylinder radius $r = 0.0061468\,\mathrm{m}$.

Figure 13 shows the contour plots for the pressure and temperature computed by the present method on a grid composed of 61 × 61 grid points. The grids are clustered in the radial direction and uniformly distributed in the angular direction. Figures 14 and 15 show results for the pressure coefficient and heat transfer on the surface of the body, respectively. It can be seen that the present results compare very well with the spectral solution.

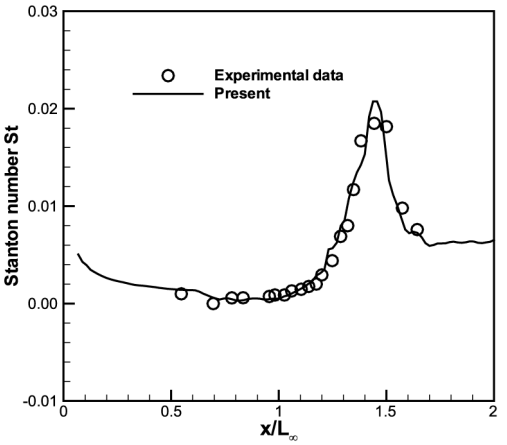

Figure 12.
Stanton number for hypersonic flow past 24° ramp

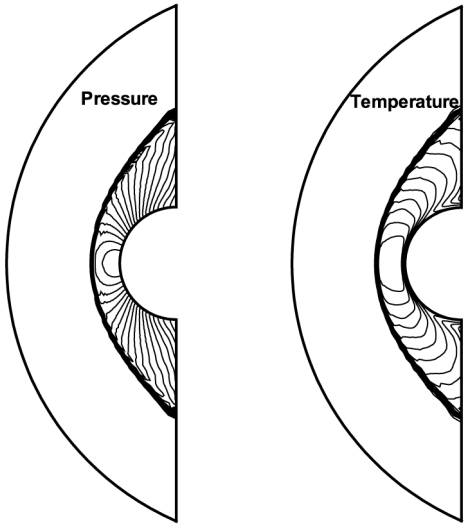

Figure 13.
Pressure and temperature contours for hypersonic flow past circular cylinder

Conclusions

A fourth-order compact method is developed for solving the two-dimensional Navier-stokes equations. The method is based on the AUSM flux splitting and a cell-centered compact scheme for the discretization of convective flux terms. A central compact scheme is used for the discretization of the diffusion flux terms. The numerical method is tested by solving four example problems, namely, the laminar boundary layer past a flat plate and the problem of shock/boundary layer interaction. The tests have shown good agreement with theoretical and experimental data. The inadequacy of the conventional FVS for solving Navier-Stokes equations is also demonstrated.

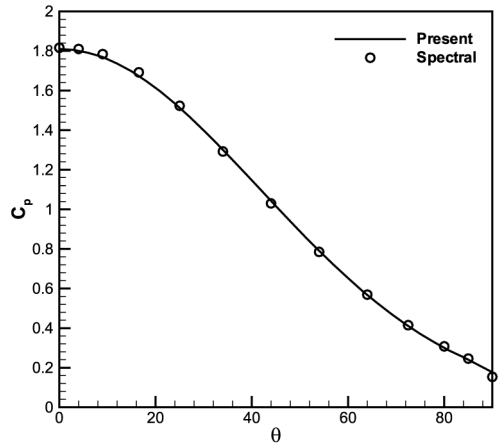

Figure 14.
Pressure coefficient C_p for hypersonic flow past circular cylinder

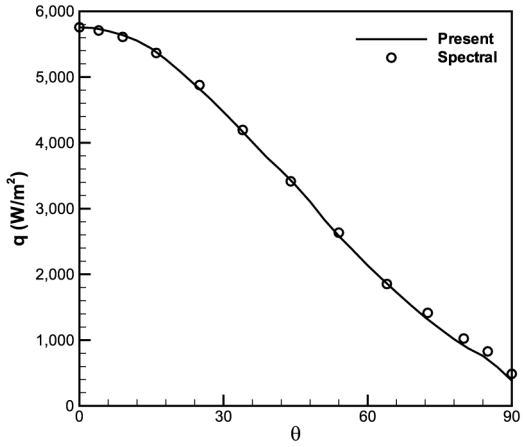

Figure 15.
Heat transfer rate for hypersonic flow past circular cylinder

References

Cockburn, B. and Shu, C.W. (1994), "Nonlinearly stable compact schemes for shock calculation", *SIAM Journal on Numerical Analysis*, Vol. 31, pp. 607-27.

Deng, X. and Maekawa, H. (1997), "Compact high-order accurate nonlinear schemes", *Journal of Computational Physics*, Vol. 130, pp. 77-91.

Deng, X. and Zhang, H. (2000), "Developing high-order weighted compact nonlinear schemes", *Journal of Computational Physics*, Vol. 165, pp. 22-44.

Ekaterinaris, J.A. (1999), "Implicit high-resolution, compact schemes for gas dynamics and aeroacoustics", *Journal of Computational Physics*, Vol. 156, pp. 272-99.

Ekaterinaris, J.A. (2000), "Implicit high-order-accurate in-space algorithms for the Navier-Stokes equations", *AIAA Journal*, Vol. 38, pp. 1594-602.

Hakkinen, R.J., Greber, I., Trilling, L. and Abarnel, S.S. (1957), "The interaction of an oblique shock wave with laminar boundary layer", Fluid Dynamics Research Group M.I.T., TR 57-1.

Kim, K.H., Lee, J.H. and Rho, O.H. (1998), "An improved of AUSM schemes by introducing the pressure-based weight functions", *Computers & Fluids*, Vol. 27, pp. 311-46.

Kopriva, D.A. (1993), "Spectral solution of the viscous blunt-body problem", *AIAA Journal*, Vol. 31, pp. 1235-41.

Lele, S.K. (1992), "Compact finite difference schemes with spectral-like resolution", *Journal of Computational Physics*, Vol. 103, pp. 16-42.

Liou, M.S. and Steffen, C.J. (1993), "A new flux splitting scheme", *Journal of Computational Physics*, Vol. 107, pp. 23-9.

Mawlood, M.K., Asrar, W., Omar, A.A. and Basri, S. (2003), "A high-resolution compact upwind algorithm for inviscid flows", paper presented at the 41st Aerospace Sciences Meeting and Exhibit Conference, AIAA-2003-0076.

Ravichandran, K.S. (1997), "High order KFVS algorithms using compact upwind difference operators", *Journal of Computational Physics*, Vol. 130, pp. 161-73.

Roe, P.L. (1981), "Approximate Riemann solvers, parameter vectors, and difference schemes", *Journal of Computational Physics*, Vol. 43, pp. 357-72.

Steger, J.L. and Warming, R.F. (1981), "Flux vector splitting of the inviscid gas dynamics equations with application to finite difference methods", *Journal of Computational Physics*, Vol. 40, pp. 263-93.

Van Leer, B. (1979), "Towards the ultimate conservation difference scheme V. A second order sequel to Godunov's method", *Journal of Computational Physics*, Vol. 32, pp. 101-36.

Wilson, R.V., Demuran, A.O. and Carpenter, M. (1998), "High-order compact schemes for numerical simulation of incompressible flows", ICASE Report No. 9813, NASA/CR-1998-206922.

Yamamoto, S. and Daiguji, H. (1993), "Higher-order-accurate upwind schemes for solving the compressible Euler and Navier-Stokes equations", *Computers & Fluids*, Vol. 22 Nos 2/3, pp. 259-70.

Corresponding author
Shahnor Basri can be contacted at shahnor@eng.upm.edu.my